

SYNTHESIS, CHARACTERIZATION AND *IN VITRO* POTENCY OF DI-, TRI-, AND TETRA-SUBSTITUTED STILBENE DERIVATIVES AS VASORELAXANT

CHAN SOCK YING

UNIVERSITI SAINS MALAYSIA

2021

SYNTHESIS, CHARACTERIZATION AND *IN VITRO* POTENCY OF DI-, TRI-, AND TETRA-SUBSTITUTED STILBENE DERIVATIVES AS VASORELAXANT

by

CHAN SOCK YING

**Thesis submitted in fulfilment of the requirements
for the degree of
Master of Science**

May 2021

ACKNOWLEDGEMENT

First and foremost, I wish to express my deepest gratitude to my supervisor, Assoc. Prof. Dr. Oo Chuan Wei, and co-supervisor, Assoc. Prof. Dr. Yam Mun Fei, who gave me the precious opportunities, inspiration and motivation to explore the research area of organic synthesis and the antihypertensive drug development. Much pleasure to have their valuable advices and guidance throughout my candidature period. I would also like to express my gratitude to Dr. Loh Yean Chun, who taught and helped me a lot in especially the bioassay part of my project. Besides, I would like to extend my warmest thanks to my seniors, Ms. Ong Hoay Ching and Mr. Tan Khai Chen for their useful opinions and guidance in my thesis writing. I would like to acknowledge the staffs of School of Chemical Sciences, USM especially Mdm Wan Zulilawati and Ms Alia Syazana for assisting me in using the research facilities. I truly appreciate the research funds from the Fundamental Research Grant Scheme, FRGS (203/PKIMIA/6711793) allocated by the Ministry of Higher Education Malaysia to my project. There is no word can express my gratitude to my parents, my love ones and my friends for their continuous encouragement and support throughout my study. To my deceased teacher, Puan Wong Po Po, thank you for teaching me how to draw my first benzene ring, your way to give STPM students motivation and inspiration was truly awesome. To my dad, my family and NLC, who groom my identity and restored my confidence, thank you for your endless patience and love.

TABLE OF CONTENTS

ACKNOWLEDGEMENT.....	ii
TABLE OF CONTENTS.....	iii
LIST OF TABLES	vi
LIST OF FIGURES	ix
LIST OF SCHEMES	xi
LIST OF SYMBOLS AND UNITS.....	xiii
LIST OF ABBREVIATIONS	xiv
LIST OF APPENDICES	xvii
ABSTRAK	xix
ABSTRACT.....	xx
CHAPTER 1 INTRODUCTION	1
1.1 Stilbene and Stilbenoids	1
1.2 Examples of Some Bioactive Stilbenoids	3
1.2.1 Resveratrol	3
1.2.2 Pterostilbene	5
1.2.3 Gnetol	6
1.2.4 Piceatannol.....	6
1.2.5 Combretastatin A-4.....	7
1.3 Chemical Synthesis Approaches of Stilbene Derivatives	7
1.3.1 Wittig reaction	8
1.3.2 Horner-Wadsworth-Emmons reaction.....	9
1.3.3 Heck reaction	10
1.3.4 Perkin reaction	11
1.3.5 Knoevenagel condensation	12
1.3.6 Modified Julia olefination.....	12
1.4 Blood Vessel and Hypertension	13
1.4.1 Vascular tone and general mechanism of vasorelaxation.....	15
1.5 Potential Medications for Hypertension.....	16
1.5.1 Vasorelaxants.....	16
1.6 Stilbene Derivatives as Potential Vasorelaxants	17
1.7 Problem Statement	19
1.8 Objectives of the Research.....	20
1.9 Scope of Study	20

CHAPTER 2 METHODOLOGY	21
2.1 Materials.....	21
2.2 Characterization of the Synthesized Compounds.....	23
2.2.1 Melting points	23
2.2.2 Fourier Transform Infrared (FT-IR) Spectroscopy.....	23
2.2.3 Fourier Transform Nuclear Magnetic Resonance (FT-NMR) Spectroscopy	23
2.3 Synthesis of Stilbene Derivatives.....	24
2.3.1 Synthesis of phosphonium salts (18a-m) from dihydroxybenzoic acids, (12a-e) and methoxybenzaldehydes, (15f-m)	25
2.3.1(a) Synthesis of ethyl dihydroxybenzoate (13a-e).....	26
2.3.1(b) Synthesis of ethyl diethoxybenzoate (14a-e).....	26
2.3.1(c) Synthesis of (alkoxyphenyl)methanol (16a-m).....	26
2.3.1(d) Synthesis of (chloromethyl)alkoxybenzene (17a-m).....	27
2.3.1(e) Synthesis of chloro(alkoxybenzyl)triphenyl- λ^5 -phosphane (18a-m).....	27
2.3.2 Synthesis of tri-ethoxy stilbene derivatives, SB 1a-7a	31
2.3.3 Synthesis of tetra-methoxy stilbene derivatives, SB 8a-13a	34
2.3.4 Synthesis of di-methoxy stilbene derivatives, SB 14-16	36
2.3.5 Synthesis of hydroxylated stilbene derivatives , SB 1b , SB 3b-4b , SB 6b-8b and SB 11b-13b	41
2.4 Bioassay	46
2.4.1 Stock solution preparation	47
2.4.2 Aortic rings preparation	47
2.4.3 Vascular response of stilbene derivatives	48
2.4.4 Statistical analysis.....	48
CHAPTER 3 RESULTS AND DISCUSSION.....	49
3.1 Reaction Mechanisms of Syntheses	49
3.2 Hyperconjugative pi Bonding of Phosphonium Salt.....	53
3.3 Tri-ethoxy Stilbene Derivatives, SB 1a-7a	53
3.3.1 Physical characterization	53
3.3.2 Fourier transform infrared spectroscopy (FT-IR).....	54
3.3.3 Fourier transform nuclear magnetic resonance spectroscopy (FT-NMR).....	57
3.4 Tetra-methoxy Stilbene Derivatives, SB 8a-13a.....	75
3.4.1 Physical characterization	75

3.4.2	Fourier transform infrared spectroscopy (FT-IR).....	75
3.4.3	Fourier transform nuclear magnetic resonance spectroscopy (FT-NMR).....	78
3.5	Di-methoxy Stilbene Derivatives, SB 14-16.....	93
3.5.1	Physical characterization	93
3.5.2	Fourier transform infrared spectroscopy (FT-IR).....	93
3.5.3	Fourier transform nuclear magnetic resonance spectroscopy (FT-NMR).....	96
3.6	Hydroxylated Stilbene Derivatives, SB 1b, 3b-4b, 6b-8b, 11b-13b	108
3.6.1	Physical characterization	108
3.6.2	Fourier transform infrared spectroscopy (FT-IR).....	108
3.6.3	Fourier transform nuclear magnetic resonance spectroscopy (FT-NMR).....	110
3.7	Vasoactivity Screening by <i>In Vitro</i> Aortic Rings Assay	117
3.8	Preliminary Structure-activity Relationship Analysis.....	120
	CHAPTER 4 CONCLUSION AND FUTURE RECOMMENDATIONS	122
4.1	Conclusion.....	122
4.2	Recommendations for Future Research	123
	REFERENCES.....	124
	APPENDICES	
	LIST OF PUBLICATIONS AND CONFERENCE	

LIST OF TABLES

	Page
Table 1.1	American Heart Association (AHA) guidelines of hypertension [Bakris et al. 2019].....14
Table 2.1	List of chemicals used in the synthesis (Section 2.3).....21
Table 2.2	List of chemicals used in the bioassay (Section 2.4).....22
Table 2.3	The chemical structure of the stilbene derivatives, SB 1a-16 with their respective reactants : phosphonium salt and substituted benzaldehyde.....38
Table 2.4	The chemical structures of the stilbene derivatives, SB 1b, SB 3b-4b, SB 6b-8b and SB 11-13b45
Table 3.1	The percentage yields, color and melting points of tri-ethoxy stilbene derivatives, SB 1a-7a 53
Table 3.2	FT-IR functional groups and the corresponding wavenumbers of tri-ethoxy stilbene derivatives , SB 1a-7a56
Table 3.3	The relative position of the coupled protons on the A-rings of SB 1a-7a with their respective splitting patterns at 500 MHz.....61
Table 3.4	The relative position of the coupled protons on the B-rings of SB 6a-7a with their respective splitting patterns at 500 MHz.....62
Table 3.5	¹ H- ¹ H correlations as inferred from 2D COSY experiment for SB 1a-7a 64
Table 3.6	Chemical shifts, δ/ppm and proton assignments of SB 1a-7a65
Table 3.7	¹ H- ¹³ C correlations as inferred from 2D HMQC experiment for SB 1a-7a70
Table 3.8	¹ H- ¹³ C correlations as inferred from 2D HMBC experiment for SB 1a-7a71
Table 3.9	Chemical shifts, δ/ppm and carbon atom assignments of SB 1a-7a73

Table 3.10	The percentage yields, color and melting points of tetra-methoxy stilbene derivatives , SB 8a-13a	75
Table 3.11	FT-IR functional groups and the corresponding wavenumbers of tetra-methoxy stilbene derivatives , SB 8a-13a	77
Table 3.12	¹ H- ¹ H correlations as inferred from 2D COSY experiment for SB 8a-13a	82
Table 3.13	Chemical shifts, δ/ppm and proton assignments of SB 8a-13a	83
Table 3.14	¹ H- ¹³ C correlations as inferred from 2D HMQC experiment for SB 8a-13a	88
Table 3.15	¹ H- ¹³ C correlations as inferred from 2D HMBC experiment for SB 8a-13a	89
Table 3.16	Chemical shifts, δ/ppm and carbon atom assignments of SB 8a-13a	91
Table 3.17	The percentage yields, color and melting points of di-methoxy stilbene derivatives , SB 14-16	93
Table 3.18	FT-IR functional groups and the corresponding wavenumbers of di-methoxy stilbene derivatives , SB 14-16	95
Table 3.19	¹ H- ¹ H correlations as inferred from 2D COSY experiment for SB 14-16	100
Table 3.20	Chemical shifts, δ/ppm and proton assignments of SB 14-16	101
Table 3.21	¹ H- ¹³ C correlations as inferred from 2D HMQC experiment for SB 14-16	105
Table 3.22	¹ H- ¹³ C correlations as inferred from 2D HMBC experiment for SB 14-16	106
Table 3.23	Chemical shifts, δ/ppm and carbon atom assignments of SB 14-16	107
Table 3.24	The percentage yields, color and melting points hydroxylated stilbene derivatives , SB 1b, SB 3b, SB 4b, SB 6b-8b and SB 11b-13b	108

Table 3.25	FT-IR functional groups and the corresponding wavenumbers of hydroxylated stilbene derivatives, SB 1b , SB 3b , SB 4b , SB 6b-8b , SB 11b-13b	110
Table 3.26	Chemical shifts, δ /ppm and proton assignments of SB 1b , 3b-4b , 6b-8b and 11b-13b	113
Table 3.27	Chemical shifts, δ /ppm and carbon atom assignments of SB 1b , 3b-4b , 6b-8b and 11b-13b	115
Table 3.28	The maximum relaxation (R_{max}) value of the endothelium-intact isolated aortic rings in response to the synthesized stilbene derivatives, SB 1a-13a , SB 14-16 and SB 1b , 3b-4b , 6b-8b , 11b-13b	118

LIST OF FIGURES

	Page
Figure 1.1	General structure and numbering system of the <i>trans</i> - (<i>E</i>) stilbenoid [Jung et al. 2009].....2
Figure 1.2	Example of the dimer of stilbenoid, δ -viniferin (2) [Xiao et al. 2008].....2
Figure 1.3	The chemical structure of resveratrol (3).....4
Figure 1.4	<i>Veratrum grandiflorum</i> sp. [Ree 2008] where 3 was first isolated.....4
Figure 1.5	The chemical structure of pterostilbene (4).....6
Figure 1.6	The chemical structure of gnetol (5)..... 6
Figure 1.7	The chemical structure of piceatannol (6).....7
Figure 1.8	The chemical structure of combretastatin A-4 (7)..... 7
Figure 1.9	Cross section diagram of the artery [Thomas and Sumam 2016].....14
Figure 1.10	Vasorelaxation mechanism in blood vessels [Vranken and Weiss 2013]..... 16
Figure 1.11	The chemical structures of hydralazine (10) and minoxidil (11).....17
Figure 2.1	The organ bath set up 47
Figure 3.1	FT-IR spectrum of SB 1a55
Figure 3.2	¹ H NMR spectrum of SB 1a (CDCl ₃)..... 58
Figure 3.3	Expanded FT-NMR spectra of SB 1a-7a at δ 6.30-7.70 ppm (CDCl ₃)..... 59
Figure 3.4	Resonances structure of tri-ethoxy stilbene derivatives..... 60
Figure 3.5	Expanded ¹ H COSY spectrum of SB 1a (CDCl ₃).....63

Figure 3.6	¹³ C NMR spectrum of SB 1a (CDCl ₃).....	68
Figure 3.7	Expanded ¹ H- ¹³ C HMQC spectrum of SB 1a (CDCl ₃).....	69
Figure 3.8	Expanded ¹ H- ¹³ C HMBC spectrum of SB 1a (CDCl ₃).....	69
Figure 3.9	FT-IR spectrum of SB 8a	76
Figure 3.10	¹ H NMR spectrum of SB 8a (CDCl ₃).....	79
Figure 3.11	Expanded FT-NMR spectra of SB 8a-13a at δ 6.20-7.60 ppm (CDCl ₃).....	80
Figure 3.12	Expanded ¹ H COSY spectrum of SB 8a (CDCl ₃).....	81
Figure 3.13	¹³ C NMR spectrum of SB 8a (CDCl ₃).....	86
Figure 3.14	Expanded ¹ H- ¹³ C HMQC spectrum of SB 8a (CDCl ₃).....	87
Figure 3.15	Expanded ¹ H- ¹³ C HMBC spectrum of SB 8a (CDCl ₃).....	87
Figure 3.16	FT-IR spectrum of SB 14	94
Figure 3.17	¹ H NMR spectrum of SB 14 (CDCl ₃).....	97
Figure 3.18	Expanded FT-NMR spectra of SB 14-16 at δ 6.60-7.60 ppm (CDCl ₃).....	98
Figure 3.19	Expanded ¹ H COSY spectrum of SB 14 (CDCl ₃).....	99
Figure 3.20	¹³ C NMR spectrum of SB 14 (CDCl ₃).....	103
Figure 3.21	Expanded ¹ H- ¹³ C HMQC spectrum of SB 14 (CDCl ₃).....	104
Figure 3.22	Expanded ¹ H- ¹³ C HMBC spectrum of SB 14 (CDCl ₃).....	104
Figure 3.23	FT-IR spectrum of SB 1b	109
Figure 3.24	¹ H NMR spectrum of SB 1b (DMSO-d ₆).....	111
Figure 3.25	¹³ C NMR spectrum of SB 1b (DMSO-d ₆).....	112
Figure 3.26	The R _{max} comparison chart of the RV with SB compounds.....	119

LIST OF SCHEMES

	Page
Scheme 1.1	Photoisomerization of the stilbene skeleton [Görner and Kuhn 1994]..... 1
Scheme 1.2	Biosynthesis of 3 5
Scheme 1.3	The Wittig reaction mechanism [Byrne and Gilheany 2013]..... 8
Scheme 1.4	The stereoselectivity-determining step of Wittig reaction [Robiette et al. 2005; Robiette et al. 2006]..... 9
Scheme 1.5	Synthesis of 3 via HWE reaction [Fan et al. 2010]..... 10
Scheme 1.6	Synthesis of 3 via Heck reaction [Fan et al. 2010]..... 10
Scheme 1.7	Synthesis of 7 via Perkin reaction [Gaukrager et al. 2001]..... 11
Scheme 1.8	Synthesis of 3 via microwave-assisted Perkin reaction [Sinha et al. 2007]..... 12
Scheme 1.9	Synthesis of unsymmetrical (<i>E</i>)-stilbenes comprising a cyano group (9) via Knoevenagel reaction [Al-Shihry 2004]..... 12
Scheme 1.10	Synthesis of 3 via modified Julia Olefination [Shenvi et al. 2016]..... 13
Scheme 2.1	The synthesis of phosphonium salts, (18a-m). Reagents and conditions: i) EtOH, H ₂ SO ₄ , reflux; ii) bromoethane, K ₂ CO ₃ , KI, acetone, reflux; iii) NaBH ₄ , THF-MeOH, reflux; iv) SOCl ₂ , pyridine, r.t ; v) triphenylphosphine, THF, 120°C 25
Scheme 2.2	The synthesis of tri-ethoxy stilbene derivatives, SB 1a-7a . Reagents and conditions: NaOH, DCM, reflux 31
Scheme 2.3	The synthesis of tetra-methoxy stilbene derivatives, SB 8a-13a . Reagents and conditions: NaOH, DCM, reflux 34
Scheme 2.4	The synthesis of di-methoxy stilbene derivatives, SB 14-16 . Reagents and conditions: NaOH, DCM, reflux..... 36

Scheme 2.5	The synthesis of hydroxylated stilbene derivative, SB 1b . Reagents and conditions: AlCl ₃ , PhNMe ₂ , 180 °C.....	41
Scheme 3.1	Reaction mechanism for synthesis of 18a from 14a	50
Scheme 3.2	Reaction mechanism for synthesis of SB 1a	51
Scheme 3.3	Reaction mechanism for synthesis of SB 1b	52

LIST OF SYMBOLS AND UNITS

δ	Chemical shift
J	Coupling constant
$^{\circ}\text{C}$	Degree Celsius
g	Gram
Hz	Hertz
h	hour
<	Less than
MHz	Megahertz
μL	Microlitre
mg	Milligram
mL	Millilitre
mm	Millimetre
mmHg	Millimetre of mercury
mM	Millimolar
mmol	Millimole
mins	Minutes
M	Molarity
>	More than
ppm	Parts per million
%	Percentage
g mol^{-1}	Unit of molar mass
cm^{-1}	Wavenumber

LIST OF ABBREVIATIONS

COSY	^1H - ^1H correlation spectroscopy
Ac ₂ O	Acetic anhydride
Ach	Acetylcholine chloride
AHF	Acute heart failure
AlCl ₃	Aluminium Trichloride
AHA	American Heart Association
ANOVA	Analysis of variance
AR	Analytical reagent
ACE	Angiotensin-converting enzyme
ATR	Attenuated Total Reflectance
S _N 2	Bimolecular nucleophilic substitution
BBr ₃	Boron Tribromide
BCl ₃	Boron Trichloride
br	Broad
CaCl ₂	Calcium chloride
Ca ²⁺	Calcium ion
CO ₂	Carbon dioxide
¹³ C NMR	Carbon-13 nuclear magnetic resonance
CVD	Cardiovascular diseases
Cu	Copper
cGMP	Cyclic guanosine monophosphate
CDCl ₃	Deuterated chloroform
DMSO-d ₆	Deuterated dimethyl sulfoxide
DCM	Dichloromethane
DMAC	Dimethylacetamide
d	Doublet
dd	Doublets of Doublet
dt	Doublets of Triplet
eNOS	Endothelial nitric oxide synthase

EDRFs	Endothelium-derived relaxing factors
equiv.	Equivalent
EtOH	Ethanol
FT-IR	Fourier-transform infrared spectroscopy
GTP	Guanosine triphosphate
GC	Guanylate cyclase
EC ₅₀	Half maximal effective concentration
HMBC	Heteronuclear Multiple Bond Correlation
HMQC	Heteronuclear Multiple-Quantum Correlation
HWE	Horner-Wadsworth-Emmons
H ₂ O ₂	Hydrogen peroxide
¹ H NMR	Hydrogen-1 nuclear magnetic resonance
IP ₃	Inositol 1,4,5-triphosphate
Krebs	Krebs-Henseleit solution
PE	L(-)-Phenylephrine
MgSO ₄	Magnesium sulphate
R _{max}	Maximal relaxation value
MeOH	Methanol
MW	Microwave
m	Multiplet
Cy ₂ NMe	<i>N,N</i> -Dicyclohexylmethylamine
PhNMe ₂	<i>N,N</i> -Dimethylaniline
NO	Nitric oxide
NOS	Nitric oxide synthase
1D NMR	One-dimensional nuclear magnetic resonance
O ₂	Oxygen
Pd(OAc) ₂	Palladium(II) acetate
³¹ P NMR	Phosphorus-31 nuclear magnetic resonance
PEG	Polyethylene Glycol
K ₂ CO ₃	Potassium carbonate
KCl	Potassium chloride
KH ₂ PO ₄	Potassium dihydrogen phosphate

KI	Potassium Iodide
K ⁺	Potassium ion
K ₃ PO ₄	Potassium phosphate
PKG	Protein Kinase I
q	Quadruplet
RV	Resveratrol
r.t.	Room temperature
SR	Sarcoplasmic reticulum
s	Singlet
NaHCO ₃	Sodium bicarbonate
NaBH ₄	Sodium borohydride
NaCl	Sodium chloride
NaH	Sodium hydride
NaOH	Sodium hydroxide
Na ₂ WO ₄ ·2H ₂ O	Sodium tungstate dihydrate
SHHF	Spontaneous hypertensive heart failure
SHR	Spontaneous hypertensive rat
SD	Sprague Dawley
S.E.M.	Standard error of mean
SAR	Structure-activity relationship
H ₂ SO ₄	Sulfuric acid
THF	Tetrahydrofuran
TBAB	Tetra- <i>n</i> -butylammonium bromide
SOCl ₂	Thionyl Chloride
NEt ₃	Triethylamine
Ph ₃ P=O	Triphenylphosphine oxide
t	Triplet
td	Triplets of Doublet
2D NMR	Two-dimensional nuclear magnetic resonance
VSMCs	Vascular smooth muscles
H ₂ O	Water

LIST OF APPENDICES

APPENDIX 1	¹ H NMR SPECTRUM OF 18a (DMSO-d ₆)
APPENDIX 2	¹ H NMR SPECTRUM OF 18b (DMSO-d ₆)
APPENDIX 3	¹ H NMR SPECTRUM OF 18c (DMSO-d ₆)
APPENDIX 4	¹ H NMR SPECTRUM OF 18d (DMSO-d ₆)
APPENDIX 5	¹ H NMR SPECTRUM OF 18e (DMSO-d ₆)
APPENDIX 6	¹ H NMR SPECTRUM OF 18f (DMSO-d ₆)
APPENDIX 7	¹ H NMR SPECTRUM OF 18g (DMSO-d ₆)
APPENDIX 8	¹ H NMR SPECTRUM OF 18h (DMSO-d ₆)
APPENDIX 9	¹ H NMR SPECTRUM OF 18i (DMSO-d ₆)
APPENDIX 10	¹ H NMR SPECTRUM OF 18j (DMSO-d ₆)
APPENDIX 11	¹ H NMR SPECTRUM OF 18k (DMSO-d ₆)
APPENDIX 12	¹ H NMR SPECTRUM OF 18l (DMSO-d ₆)
APPENDIX 13	¹ H NMR SPECTRUM OF 18m (DMSO-d ₆)
APPENDIX 14	¹ H NMR SPECTRUM OF SB 2a (CDCl ₃)
APPENDIX 15	¹³ C NMR SPECTRUM OF SB 2a (CDCl ₃)
APPENDIX 16	¹ H NMR SPECTRUM OF SB 3a (CDCl ₃)
APPENDIX 17	¹³ C NMR SPECTRUM OF SB 3a (CDCl ₃)
APPENDIX 18	¹ H NMR SPECTRUM OF SB 4a (CDCl ₃)
APPENDIX 19	¹³ C NMR SPECTRUM OF SB 4a (CDCl ₃)
APPENDIX 20	¹ H NMR SPECTRUM OF SB 5a (CDCl ₃)
APPENDIX 21	¹³ C NMR SPECTRUM OF SB 5a (CDCl ₃)
APPENDIX 22	¹ H NMR SPECTRUM OF SB 6a (CDCl ₃)
APPENDIX 23	¹³ C NMR SPECTRUM OF SB 6a (CDCl ₃)
APPENDIX 24	¹ H NMR SPECTRUM OF SB 7a (CDCl ₃)
APPENDIX 25	¹³ C NMR SPECTRUM OF SB 7a (CDCl ₃)
APPENDIX 26	¹ H NMR SPECTRUM OF SB 9a (CDCl ₃)
APPENDIX 27	¹³ C NMR SPECTRUM OF SB 9a (CDCl ₃)
APPENDIX 28	¹ H NMR SPECTRUM OF SB 10a (CDCl ₃)

APPENDIX 29	¹³ C NMR SPECTRUM OF SB 10a (CDCl ₃)
APPENDIX 30	¹ H NMR SPECTRUM OF SB 11a (CDCl ₃)
APPENDIX 31	¹³ C NMR SPECTRUM OF SB 11a (CDCl ₃)
APPENDIX 32	¹ H NMR SPECTRUM OF SB 12a (CDCl ₃)
APPENDIX 33	¹³ C NMR SPECTRUM OF SB 12a (CDCl ₃)
APPENDIX 34	¹ H NMR SPECTRUM OF SB 13a (CDCl ₃)
APPENDIX 35	¹³ C NMR SPECTRUM OF SB 13a (CDCl ₃)
APPENDIX 36	¹ H NMR SPECTRUM OF SB 15 (CDCl ₃)
APPENDIX 37	¹³ C NMR SPECTRUM OF SB 15 (CDCl ₃)
APPENDIX 38	¹ H NMR SPECTRUM OF SB 16 (CDCl ₃)
APPENDIX 39	¹³ C NMR SPECTRUM OF SB 16 (CDCl ₃)
APPENDIX 40	¹ H NMR SPECTRUM OF SB 3b (DMSO-d ₆)
APPENDIX 41	¹³ C NMR SPECTRUM OF SB 3b (DMSO-d ₆)
APPENDIX 42	¹ H NMR SPECTRUM OF SB 4b (DMSO-d ₆)
APPENDIX 43	¹³ C NMR SPECTRUM OF SB 4b (DMSO-d ₆)
APPENDIX 44	¹ H NMR SPECTRUM OF SB 6b (DMSO-d ₆)
APPENDIX 45	¹³ C NMR SPECTRUM OF SB 6b (DMSO-d ₆)
APPENDIX 46	¹ H NMR SPECTRUM OF SB 7b (DMSO-d ₆)
APPENDIX 47	¹³ C NMR SPECTRUM OF SB 7b (DMSO-d ₆)
APPENDIX 48	¹ H NMR SPECTRUM OF SB 8b (DMSO-d ₆)
APPENDIX 49	¹³ C NMR SPECTRUM OF SB 8b (DMSO-d ₆)
APPENDIX 50	¹ H NMR SPECTRUM OF SB 11b (DMSO-d ₆)
APPENDIX 51	¹³ C NMR SPECTRUM OF SB 11b (DMSO-d ₆)
APPENDIX 52	¹ H NMR SPECTRUM OF SB 12b (DMSO-d ₆)
APPENDIX 53	¹³ C NMR SPECTRUM OF SB 12b (DMSO-d ₆)
APPENDIX 54	¹ H NMR SPECTRUM OF SB 13b (DMSO-d ₆)
APPENDIX 55	¹³ C NMR SPECTRUM OF SB 13b (DMSO-d ₆)

**SINTESIS, PENCIRIAN DAN POTENSI *IN VITRO* BAGI DI-, TRI-, DAN
TETRA-TERCANTUM TERBITAN STILBENA SEBAGAI
VASORELAKSAN**

ABSTRAK

Vasorelaksan ialah ubat dalam perawatan krisis hipertensi. Stilbenoid yang dikaji dengan umum, iaitu resveratrol (RV) telah dilaporkan tentang keupayaannya dalam mencetuskan vasorelaksasi pada membran salur darah melalui pelbagai laluan pengisyaratan. Dalam kajian ini, terbitan stilbena tri-etoksi (**SB 1a-7a**), tetra-metoksi (**SB 8a-13a**) dan di-metoksi (**SB 14-16**) telah berjaya disintesis melalui tindak balas konvensional Wittig di mana gelang A dan B bagi tulang belakang stilbenoid masing-masing dibentuk daripada garam fosfonium yang disintesis dan terbitan benzaldehid komersial. Isomer *trans*- (*E*) telah dipencilkan dan dituliskan. Stilbena terhidroksi (**SB 1b**, **SB 3b-4b**, **SB 6b-8b** and **SB 11b-13b**) disintesis selanjutnya daripada stilbena teralkoksi melalui kaedah poli *O*-pendealkilan menggunakan sistem aluminium triklorida/*N,N*-dimetilanilin yang diubahsuai. Semua sebatian **SB** yang disintesis telah dicirikan menggunakan spektroskopi FT-IR, NMR 1D dan 2D. Tindak balas vaskular *in vitro* bagi semua sebatian **SB** yang disintesis dinilai terutamanya pada gelang aorta endotelium-utuh yang diasingkan daripada tikus jantan Sprague Dawley (SD) dan pra-mengecut dengan fenilefrin (PE). **SB 6b** menunjukkan R_{max} yang luar biasa ($95.11 \pm 2.87\%$), iaitu lebih dua kali ganda peningkatan daripada sebatian ulung, RV ($R_{max} = 42.90 \pm 1.67\%$). Ini mencadangkan potensi **SB 6b** diterima sebagai sebatian ulung yang baharu bagi pengoptimuman ubat. Keseluruhan data menggambarkan bahawa jenis, bilangan dan kedudukan pengganti pada gelang A dan B adalah sama penting untuk mencetuskan tindak balas vasorelaksan.

**SYNTHESIS, CHARACTERIZATION AND *IN VITRO* POTENCY OF DI-,
TRI-, AND TETRA-SUBSTITUTED STILBENE DERIVATIVES AS
VASORELAXANT**

ABSTRACT

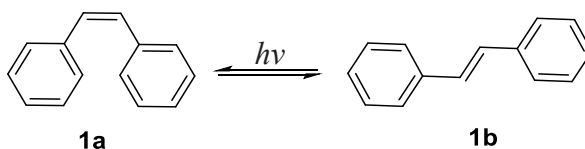
Vasorelaxant is the common drug used for the treatment of hypertensive emergencies. The most widely studied stilbenoid, namely resveratrol (**RV**) was reported its ability to induce vasorelaxation through numerous signalling pathways on the blood vessel membrane. In this study, the tri-ethoxy (**SB 1a-7a**), tetra-methoxy (**SB 8a-13a**) and di-methoxy (**SB 14-16**) stilbene derivatives were successfully synthesized via the conventional Wittig reaction wherein the A- and B- rings of the stilbene backbone were formed from the synthesized phosphonium salts and commercially available substituted benzaldehydes, respectively. The *trans*- (*E*) isomers were isolated and purified. The hydroxylated stilbenes (**SB 1b**, **SB 3b-4b**, **SB 6b-8b** and **SB 11b-13b**) were further synthesized from the alkoxyated stilbenes via poly *O*-dealkylation approach employing the modified aluminium trichloride/*N,N*-dimethylaniline system. All the synthesized **SB** compounds were elucidated by the FT-IR, 1D and 2D NMR spectroscopies. The *in vitro* vascular response of the synthesized **SB** compounds was primarily assessed on the phenylephrine (PE)-precontracted endothelium-intact isolated aortic rings of the male Sprague Dawley (SD) rats. **SB 6b** presented remarkable R_{max} (95.11 ± 2.87 %) which was more than two-fold improvement of the vasorelaxation of the lead compound, **RV** ($R_{max} = 42.90 \pm 1.67$ %), suggesting the potency of **SB 6b** to be adopted as a new lead compound for drug optimization. The overall data illustrated the type, number and position of the substituents on the A- and B-rings were equally essential in triggering the vasorelaxation response.

CHAPTER 1

INTRODUCTION

1.1 Stilbene and Stilbenoids

Stilbene is a common diarylethylene which is also known as the 1,2-diphenylethene that made up of the C6-C2-C6 backbone [Morabito et al. 2014]. The condensed structural formula of stilbene can be written as $C_6H_5CH=CHC_6H_5$ [Khishchenko et al. 2005]. It has the unique structure in which the ethylene bridge joined together the two aromatic systems; the carbon-carbon double bond restricts the free rotation therefore allowing the formation of the stereoisomers. The *cis*- (*Z*) configurations **1a** are generally less stable compared to their counterparts, the *trans*- (*E*) configurations **1b**, due to the steric hindrance existed between the two aromatic systems [Xiao et al. 2008]. Under a certain extent of the ultraviolet or visible light exposure, photoisomerization between the two isomeric forms could be observed (Scheme 1.1) [Görner and Kuhn 1994; Fan et al. 2010].



Scheme 1.1 Photoisomerization of the stilbene skeleton [Görner and Kuhn 1994].

Stilbenoids are the stilbene derivatives which further classified as the natural phenylpropanoids derived from the stilbene backbone, with different number and type of substituents bonded to different positions on the aromatic systems [Akinwumi et al. 2018]. Figure 1.1 shows the numbering system applied on the general structure of *trans*- (*E*) stilbenoid [Jung et al. 2009].

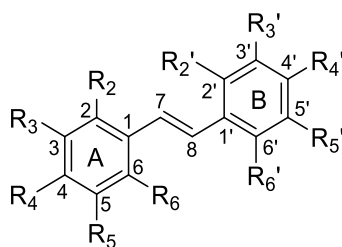


Figure 1.1 General structure and numbering system of the *trans*- (*E*) stilbenoid [Jung et al. 2009].

Stilbenoids can be found abundantly in certain specific plant families, such as the family Vitaceae, Pinaceae, Gnetaceae, Cyperaceae and Liliaceae [Almagro et al. 2013]. Stilbenoids that are formed naturally through the general phenylpropanoid pathway were originally functioned as the phytoalexin to protect the plants from pathogen infection, as well as in other abiotic stress conditions [Xiao et al. 2008; Chong et al. 2009; Akinwumi et al. 2018]. They do exist in the form of dimers, trimers, or oligomers containing the benzofuran rings recognized as the joint. δ -Viniferin (**2**) (Figure 1.2) is the general dimer of resveratrol (*(E)*-3,4',5-trihydroxystilbene) [Xiao et al. 2008; Niesen et al. 2013].

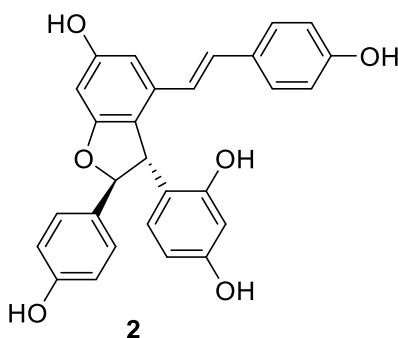


Figure 1.2 Example of the dimer of stilbenoid, δ -viniferin (**2**) [Xiao et al. 2008].

Since the last decade, stilbenoids have gained great interest in the fields of material science, photochemistry and pharmaceutical science due to their potentials to be developed into commercialized dyes, photobleachers, polymers, photoconductors, drugs, dietary supplements and molecular probes [Likhtenshtein 2012]. Many research

projects have also been conducted to reveal the chemical diversity of stilbenoids by various types and numbers of substituents available as well as different oligomeric forms to gain novel stilbenoids with improved potency in these mentioned fields [Latruffe et al. 2012].

1.2 Examples of Some Bioactive Stilbenoids

Other than the widely studied resveratrol, there are a few stilbenoids such as pterostilbene, gnetol, piceatannol, combretastatin A-4, piceid and oxyresveratrol had also been highlighted for their significant structure-activity relationships (SAR) in some biological activities [Fan et al. 2010; Latruffe et al. 2012; Akinwumi et al. 2018]. These stilbenoids have displayed a wide range of biological activities, including antihypertensive, antileukaemia, antiplatelet aggregation, anti-oxidation, antidiabetic, anti-inflammation, antimicrobial, antifungal, antilipidemic, protein-tyrosine kinase inhibitory as well as the inhibitory action on various cancer cells [Park and Pezzuto 2015; Akinwumi et al. 2018]. Although both *trans*- (*E*) and *cis*- (*Z*) configurations of stilbenoid were reported to have the significant biological properties but the *trans*- (*E*) isomers were more dominant in most of the biological activities compared to their counterparts, the *cis*- (*Z*) isomers [Akinwumi et al. 2018].

1.2.1 Resveratrol

Resveratrol (**3**), which is also known as (*E*)-3,4',5-trihydroxystilbene or (*E*)-5-(4-hydroxystyryl)benzene-1,3-diol, has two hydroxyl groups bonded to the 3- and 5-positions in A-ring and another hydroxyl group bonded to the 4'- position in B-ring (Figure 1.3) [Salehi et al. 2018]. *Trans*- (*E*) configuration of **3** is more common in nature and can be found abundantly in red grapes skin, red wine, mulberries and peanut [Rivière et al. 2012].

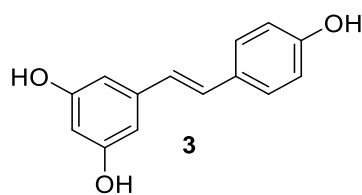


Figure 1.3 The chemical structure of resveratrol (**3**).

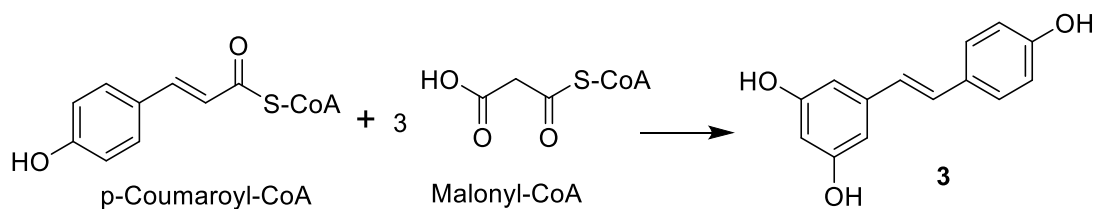
Although **3** was first isolated in 1939 from *Veratrum grandiflorum* Loes. fil. (Figure 1.4) by M. J. Takaoka but few research articles discussed about the health benefits of **3** until an epidemiologist linked the low occurrence of coronary heart diseases with the red wine consumption in France, namely the “French Paradox” in 1992 [Nakata et al. 2012; Gambini et al. 2015]. It was later found that **3** as a type of the active ingredients in red wine was effective especially in preventing the coronary diseases [Vidavalur et al. 2006].



Figure 1.4 *Veratrum grandiflorum* sp. [Ree 2008] where **3** was first isolated.

As the popularity of **3** increased tremendously, many approaches and techniques were studied and applied to develop the pure **3** into dietary supplement, including plant extraction, biosynthesis and chemical synthesis [Fan et al. 2010]. Scheme 1.2 shows the biosynthetic route to **3** from the coenzyme A derivative of

cinnamic acid [Sparvoli et al. 1994; Akinwumi et al. 2018]. Chemical synthesis of **3** and other stilbenoids were discussed in Section 1.3.



Scheme 1.2 Biosynthesis of **3**.

Although daily consumption of not more than 5 grams of **3** was considered safe for a normal adult, but the clinical data in developing **3** into drug was insufficient [Ramírez-Garza et al. 2018; Pezzuto et al. 2019]. This could be due to the unneglectable side effect of **3** in hindering blood platelet aggregation and therefore, increasing the risk of bleeding [Salehi et al. 2018]. Compound **3** was also reported to exhibit unsatisfied solubility (< 0.05 mg/mL), low oral bioavailability (20–30 %) and a very short half-life (~14 minutes) that **3** was metabolized rapidly after oral administration, contributing to its relatively low bioavailability [Akinnwumi et al. 2018; Chimento et al. 2019].

1.2.2 Pterostilbene

Pterostilbene (**4**) ((*E*)-3,5-dimethoxy-4'-hydroxystilbene), is a derivative of **3** in which the 3- and 5- hydroxyl groups in A-ring are replaced with the methoxy groups (Figure 1.5). It was known for its use in Indian Ayurvedic medicine to treat diabetes and coronary heart diseases and reported interestingly to have ~75% higher *in vivo* bioavailability and ~90 mins longer half-life than **3** [Paul et al. 1999; Akinwumi et al. 2018]. The two methoxy groups in **4** are able to enhance the membrane permeability as the alkyl moieties exhibited greater lipophilicity and could fit straightforwardly into

the ‘hydrophobic pockets’ within a targeted binding side [Giacomini et al. 2016; Tsai et al. 2017].

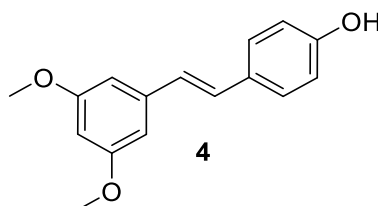


Figure 1.5 The chemical structure of pterostilbene (4).

1.2.3 *Gnetol*

Gnetol (5) ((*E*)-2,6,3',5'-tetrahydroxystilbene), extracted from the genus *Gnetum* of some gymnospermous plant has an additional hydroxyl group (Figure 1.6) compared to 3 and was reported to have unexpectedly the lower oral bioavailability (~6.5%) than resveratrol [Akinwumi et al. 2018]. It was widely used in Asia as traditional medicine for the treatment of arthritis and asthma [Remsberg et al. 2015]. The articles suggested it could be a potent tyrosinase inhibitor and arachidonic acid-induced platelet aggregation inhibitor [Ohguchi et al. 2003; Kloypan et al. 2012].

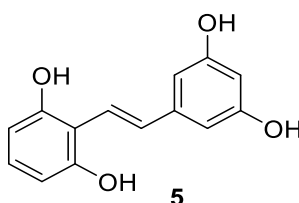


Figure 1.6 The chemical structure of gnetol (5).

1.2.4 *Piceatannol*

Piceatannol (6) ((*E*)-3,4,3',5'-tetrahydroxystilbene), as the metabolite of 3 has the hydroxyl groups in 3- and 4- positions (Figure 1.7) compared to the 2- and 6- positions of 5, was found interestingly to have 20% higher bioavailability than 3 [Akinwumi et al. 2018]. Compound 6 was reported to have a higher anti-arrhythmic

and cardioprotective effects than that of **3** in the ischaemic-reperfused rat hearts [Chen et al. 2009].

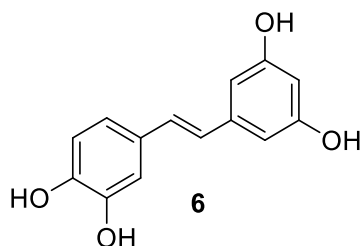


Figure 1.7 The chemical structure of piceatannol (**6**).

1.2.5 Combretastatin A-4

Combretastatin A-4 (**7**) ((*Z*)-3,4,5,4'-tetramethoxy-3'-hydroxystilbene) (Figure 1.8) isolated from *Combretum caffrum*, is a well-known anticancer agent and effective in selectively disrupting the abnormal tumour vasculature [Shan et al. 2011]. Unlike other stilbenoids in which their *trans*- isomers were more dominant, the *cis*-configuration of **7** was responsible in displaying the beneficial biological properties [Gaspari et al 2017].

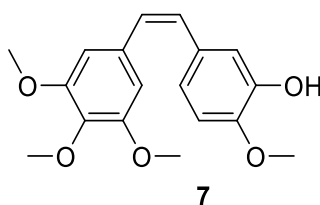


Figure 1.8 The chemical structure of combretastatin A-4 (**7**).

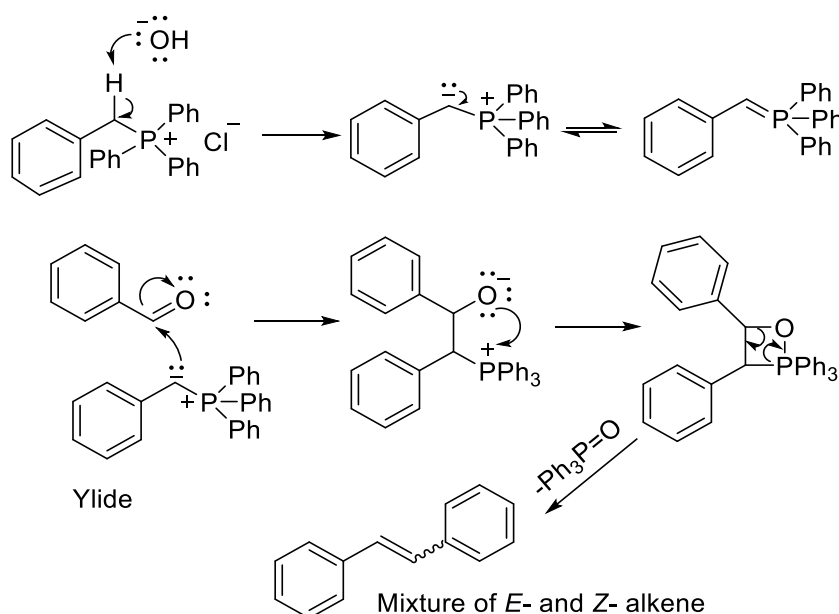
1.3 Chemical Synthesis Approaches of Stilbene Derivatives

The key step of synthesizing the stilbene backbone is the construction of the carbon-carbon double bond [Giacomini et al. 2016]. Therefore, stilbenoids can be synthesised under the Wittig, Horner-Wadsworth-Emmons (HWE), Heck and Perkin reactions, Knoevenagel condensation and modified Julia olefination. Among the mentioned chemical synthesis reactions, Wittig and Heck reactions remained as the

more widely used approaches in synthesizing the stilbenoids [Fan et al. 2010; Likhtenshtein 2012; Giacomini et al. 2016].

1.3.1 Wittig reaction

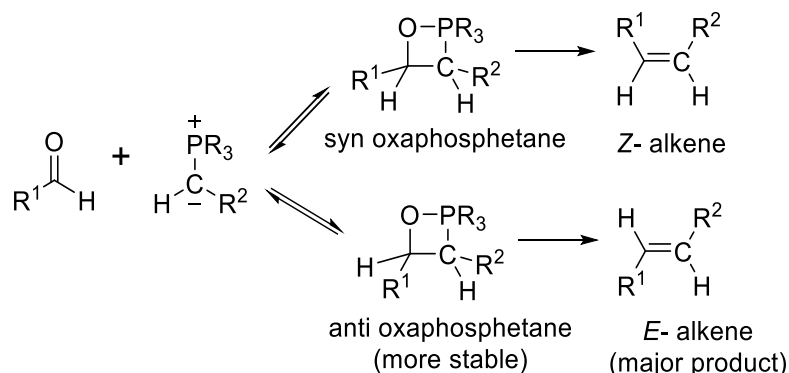
Wittig reaction was the classical approach since 1985 in transforming the aldehydes or ketones to the alkenes with the exact site of the carbon-carbon double bond [Maryanoff et al. 1985]. Generally, Wittig reaction involved the *in situ* formation of the ylide from the deprotonation of phosphonium salt by a strong base. Nucleophilic carbon of ylide (adjacent to the phosphorus atom) attacks the carbonyl carbon, forming the four membered oxaphosphetane ring followed by the elimination of the triphenylphosphine oxide [Moloney 2000]. The reaction mechanism was depicted in Scheme 1.3 [Byrne and Gilheany 2013].



Scheme 1.3 The Wittig reaction mechanism [Byrne and Gilheany 2013].

The formation of the *Z*- and *E*-alkenes is attributed to the oxaphosphetane, that arranged in either the syn- or anti-periplanar fashion. Hence, the formation of the alkenes under Wittig reaction are said to be stereospecific (Scheme 1.4). The ylides with electron donating group such as alkyl and hydroxyl are less stable but kinetically

favoured, contributing to the formation of *Z*-alkenes. Likewise, electron withdrawing groups such as aryl groups stabilize the ylides by conjugation, hence the *E*-alkenes are isolated as the major product [Robiette et al. 2005; Robiette et al. 2006].



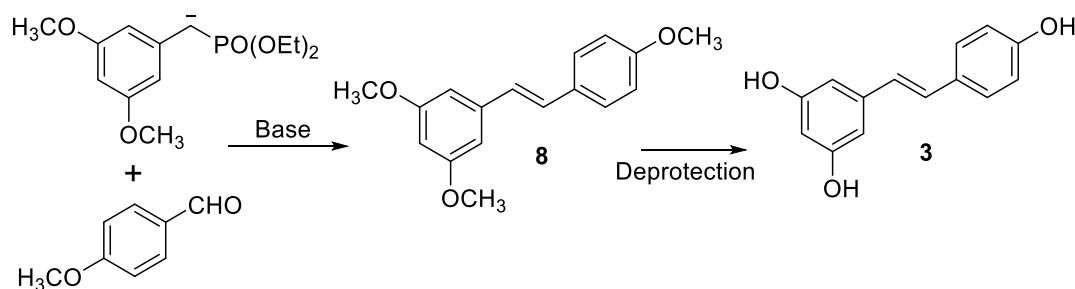
Scheme 1.4 The stereoselectivity-determining step of Wittig reaction [Robiette et al. 2005; Robiette et al. 2006].

The popularity of this reaction remains as it can be carried out under milder condition and required less expensive starting material. The main drawbacks of the reaction were the poor stereoselectivity and the difficulty in removal of the by-product, triphenylphosphine oxide [Ernst 1996]. Nevertheless, McNulty et al. [2009] had introduced the development of ylides originated from the short-chain trialkyl (i.e., ethyl and n-propyl) phosphonium salt. Their articles highlighted not only the improvement of *E*-selectivity but also the readily removal of the by-product (trialkylphosphine oxide) that is soluble in water.

1.3.2 Horner-Wadsworth-Emmons reaction

Horner-Wadsworth-Emmons (HWE) reaction was modified from the Wittig reaction, in which the more nucleophilic phosphonate-stabilized carbanions (Scheme 1.5) were preferred over phosphonium ylides. Notably, HWE reaction gave better

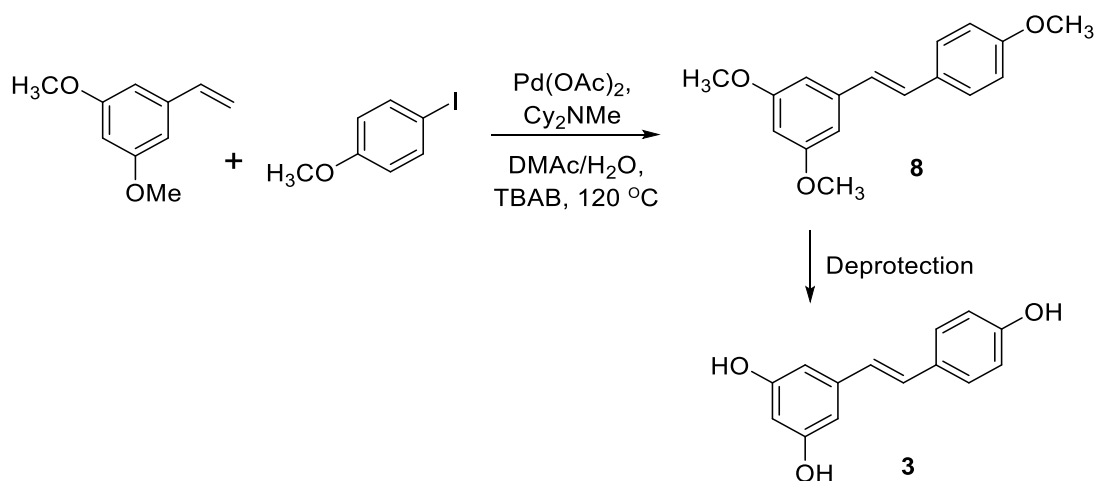
yield and *E*-selectivity compared to the conventional Wittig reaction [Maryanoff et al. 1985].



Scheme 1.5 Synthesis of **3** via HWE reaction [Fan et al. 2010].

1.3.3 Heck reaction

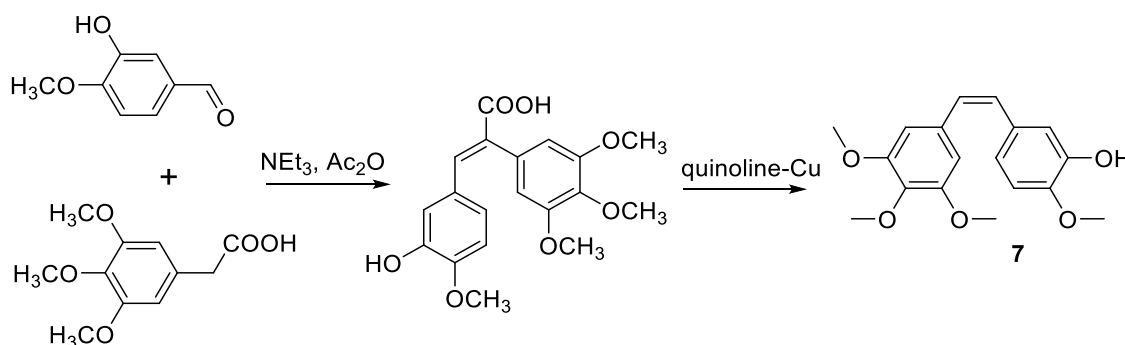
Heck reaction was well-known for its remarkable regio-, chemo-, and stereoselective characteristics [Oliveira et al. 2014; Jeffery and Ferber 2003]. Although it involves the utilizing of the higher cost palladium derived catalysts (Scheme 1.6), the fewer steps involved and higher yields in overall contributing to its popularity among researchers [Fan et al. 2010].



Scheme 1.6 Synthesis of **3** via Heck reaction [Fan et al. 2010].

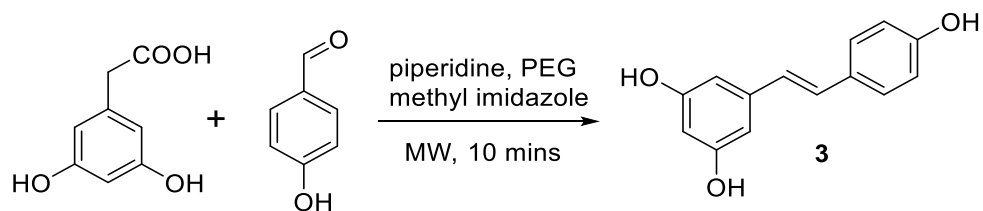
1.3.4 Perkin reaction

Conventional Perkin reaction involves four significant steps, i.e. protection, condensation, decarboxylation and deprotection. Despite the poor overall yield, it also requires relatively harsh conditions such as high temperature and toxic quinoline-Cu salt as catalyst, which in turn limit further development of the classical reaction in synthesizing stilbenoids for years [Fan et al. 2010]. However, Gaukrager et al. [2001] reported that Perkin reaction was more practical than Wittig or other reaction in synthesizing *cis*- (*Z*) stilbenoid, **7** as promising antitumor agents.



Scheme 1.7 Synthesis of **7** via Perkin reaction [Gaukrager et al. 2001].

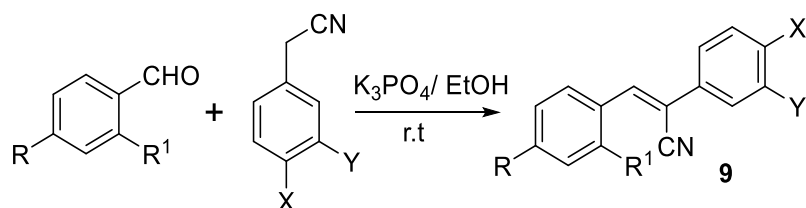
To the best of our knowledge, there was an article published in year 2007 emphasized that the one-pot preparation of stilbenoids with the improved yield of 20-50% using microwave-assisted Perkin reaction without using toxic quinoline-Cu salt as catalyst. A simultaneous condensation-decarboxylation was observed surprisingly under the modified Perkin reaction between the hydroxylated benzaldehydes and phenylacetic acids treated with piperidine-methylimidazole as the base (Scheme 1.8) [Sinha et al. 2007].



Scheme 1.8 Synthesis of **3** via microwave-assisted Perkin reaction [Sinha et al. 2007].

1.3.5 Knoevenagel condensation

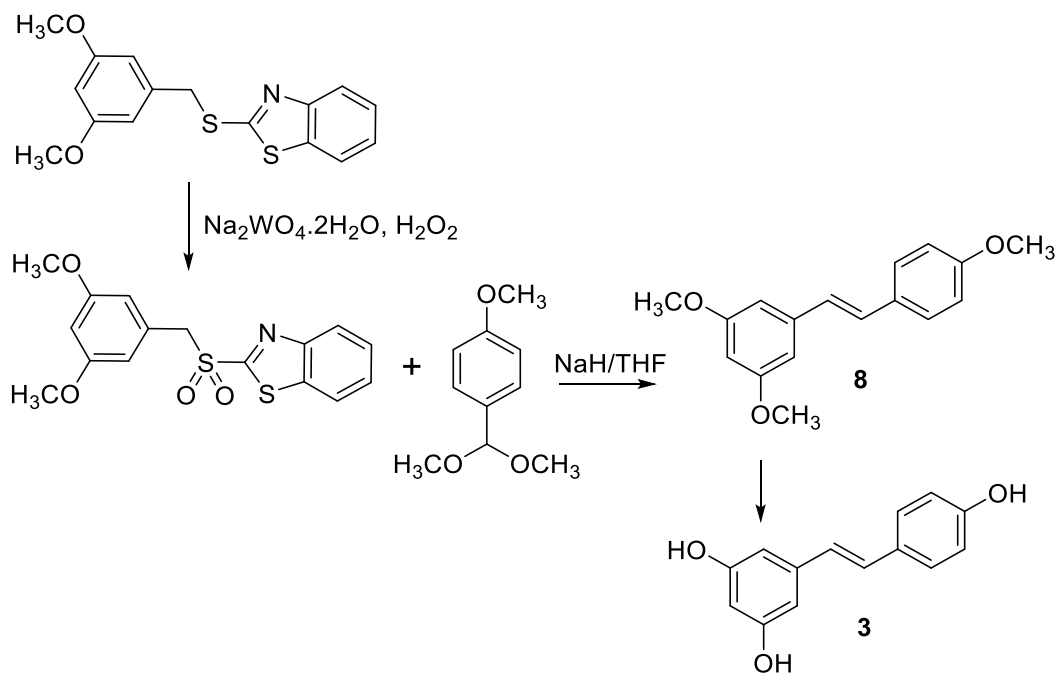
Knoevenagel condensation was used by Al-Shihry [2004] in synthesizing a few unsymmetrical (*E*)-stilbenes comprising a cyano group bonded to the sp^2 carbon of alkene at room temperature (Scheme 1.9). The reaction was reported to give only the *E*-isomers with the yield of more than 80%.



Scheme 1.9 Synthesis of unsymmetrical (*E*)-stilbenes comprising a cyano group (**9**) via Knoevenagel reaction [Al-Shihry 2004].

1.3.6 Modified Julia olefination

Under the modified Julia olefination (Scheme 1.10), the heterocyclic sulfone was added to aldehyde and gave benzothiazole sulphonyl compound which was later reacted with *p*-anisaldehyde dimethyl acetal in the presence of metallated bases. The hydroxy benzothiazole group and sulphur dioxide were removed through the Smiles rearrangement. The modified Julia olefination was reported to yield the methoxylated resveratrol (**8**) with *E*- and *Z*- isomers in a ratio of 30:70 [Shenvi et al. 2016].



Scheme 1.10 Synthesis of **3** via modified Julia Olefination [Shenvi et al. 2016].

1.4 Blood Vessel and Hypertension

Blood vessel is a tubular structure where the blood circulating inside a human's body. There are three types of blood vessels, namely arteries, veins and capillaries. Unlike the single-layered capillaries, both arteries and veins consist of three layers, i.e. tunica adventitia, tunica media and tunica intima (Figure 1.9) [Thomas and Sumam 2016]. Vasomotors, that can be found abundantly at the vascular smooth muscles (VSMCs) and endothelial cells of tunica media and tunica intima respectively, play a vital role in regulating the vascular tone that refers to the endogenous balance between the blood vessel relaxation (vasorelaxation) and contraction (vasoconstriction) [Orloff et al. 2001; Loh et al. 2018].

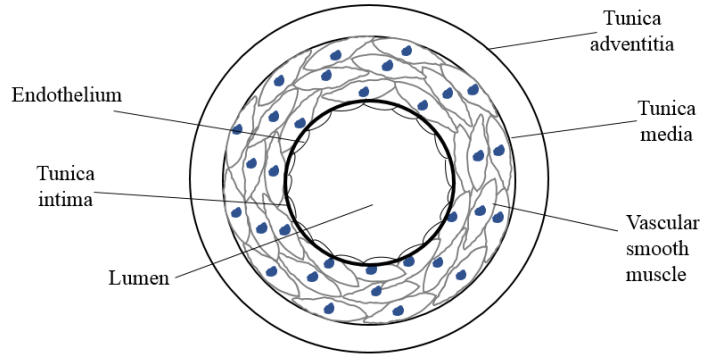


Figure 1.9 Cross section diagram of the artery [Thomas and Sumam 2016].

Blood pressure is the circulating blood force that exerted on the wall of blood vessel in human’s circulatory system [Alley and Copelin 2020]. Blood pressure can be measured from the branchial artery using the sphygmomanometer and recorded as two numbers, i.e. systolic and diastolic number, in the unit of millimetres of mercury (mm Hg) [McEniery et al. 2014]. Hypertension is a condition in which the blood pressure is recorded higher than 130 over 80 mm Hg in one’s rest state as shown in Table 1.1 [Bakris et al. 2019].

Table 1.1 American Heart Association (AHA) guidelines of hypertension [Bakris et al. 2019].

	Systolic (mm Hg)	Diastolic (mm Hg)
Normal Blood Pressure	< 120	< 80
Elevated	120-129	< 80
Stage 1 hypertension	130-139	80-89
Stage 2 hypertension	≥ 140	≤ 90
Hypertensive crisis	> 180	> 120

The causes of hypertension are closely related to one’s lifestyle, diet and environmental factors. The persistently elevated blood pressure had been proven its possibilities in triggering human cardiovascular diseases (CVD), including stroke, coronary artery disease, acute heart failure (AHF), heart attack, angina, peripheral

vascular disease, aneurysm, atrial fibrillation as well as kidney failure [McNaughton et al. 2012; Drozd et al. 2014]. Hypertensive emergencies refer to the malignant hypertension associated with the mentioned hemodynamic problems that can occur in patients who have poor control on their blood pressure as well as the uninstructed discontinued of antihypertensive medications. Severe headache, nausea, blurred vision and mental confusion are the classic symptoms of hypertensive emergencies. The symptoms may proceed with convulsions, coma, and even death. The common medication used to overcome the hypertensive emergencies is vasorelaxant in which the cardiac rate and vascular resistance could be reduced rapidly within a few hours [Benowitz et al. 2012].

1.4.1 Vascular tone and general mechanism of vasorelaxation

The arteriolar and venous tones are essential in controlling the systolic and diastolic wall stress as well as to regulate the smooth muscle tension. The general vasorelaxation mechanism is illustrated in Figure 1.10 [Vranken and Weiss 2013]. Endothelial cells are responsible in generating the nitric oxides (NO) from a specific amino acid, L-arginine through the nitric oxide synthase (NOS). NO that diffuses spontaneously away from the endothelial cell and into the adjacent smooth muscle cells activates the guanylate cyclase (GC) to transform the guanosine triphosphate (GTP) into the cyclic guanosine monophosphate (cGMP). Phosphorylation of the calcium channels occurs right after cGMP binds to the cGMP-dependent protein kinase I (PKG) as well as inhibits these channels from opening even in the presence of inositol 1,4,5-triphosphate (IP₃). Vasorelaxation takes place as the contraction of the smooth muscle is restrained due to the reduced concentration of calcium ions, Ca²⁺.

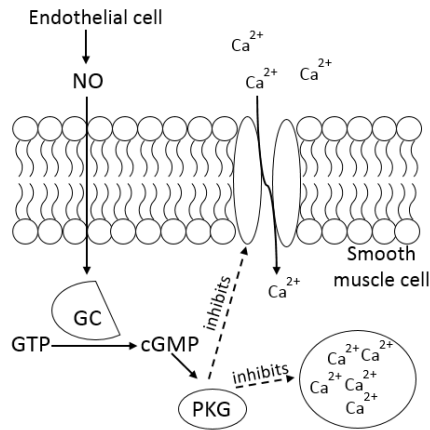


Figure 1.10 Vasorelaxation mechanism in blood vessels [Vranken and Weiss 2013].

1.5 Potential Medications for Hypertension

An approximately 1.13 billion people worldwide and 67% of Malaysian adults were diagnosed with hypertension in 2019 [Mahadir et al. 2019]. Owing to no obvious symptoms shown, most of the patients are not aware of its urgency of the persistently elevated hypertension that are always related to the chronic heart diseases [Alley and Copelin 2020]. More than 200 medications are used in the treatment of hypertension. They can be categorised into diuretics, vasorelaxants (vasodilators), angiotensin-converting enzyme (ACE) inhibitors, peripheral adrenergic inhibitors, angiotensin receptor blockers, alpha-blockers, beta-blockers, calcium channel blockers and central agonists [Kolck et al. 2004]. Other than diuretics, vasorelaxants are the second common medication for acute heart failure (AHF) as well as some hypertensive emergencies [Metra et al. 2009; Singh et al. 2017].

1.5.1 Vasorelaxants

Vasorelaxants refer to the chemical compounds that stipulate a rapid effect on the vessel walls by widening the blood vessels to increase the capacitance and reducing the obstruction effects to allow the blood to flow smoothly [Altermann et al. 2015]. Commercially available pharmaceutical medicine such as hydralazine and minoxidil

are the common vasorelaxants (Figure 1.11) [Cohn et al. 2011]. The mechanism of actions of the mentioned vasorelaxants are not necessary the same. Hydralazine released nitric oxide as the activator of soluble GC while minoxidil is responsible in preventing depolarization of smooth muscle cell membrane through the opening of potassium channels [Katzung 2012].

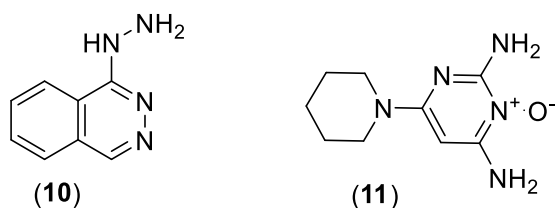


Figure 1.11 The chemical structures of hydralazine (10) and minoxidil (11).

Apart from that, certain vasorelaxants could increase the cGMP and cAMP while decreasing the intracellular calcium ions [Katzung 2012]. In fact, there are a few classes of natural compounds such as alkaloids, flavonoids, terpenoids and stilbenoids had been reported their remarkable *in vivo* and *in vitro* vasorelaxation activities as well as their mechanisms of action [Luna-Vázquez et al. 2013; Akinwumi et al. 2017; Tan et al. 2020]. These compounds trigger the vasorelaxation of smooth muscle mainly through the activation of the NO/cGMP, PGI₂/cAMP pathways, the stimulation of K⁺ channels and the blockage of voltage-dependent calcium channels. Collaborations of two or more mechanisms are crucial in showing the vasorelaxation effect [Luna-Vázquez et al. 2013].

1.6 Stilbene Derivatives as Potential Vasorelaxants

The earlier systematic studies of the vasoactive stilbene derivatives could be found way back in 2007 published by Yoo et al. where **6** (page 7) was found to have the most potent EC₅₀ compared to **3** (page 4) and another two bulky stilbene derivatives (desoxyrhapontigenin and **2**). The same article revealed that the bulky stilbenes

glucoside displayed the modest EC₅₀ in relaxing the of Sprague-Dawley (SD) rats' aorta rings. In the aspect of the studied mechanism, **3** and **6** were reported effective in activating and regulating endothelial NO synthase (eNOS) on rat's aorta and mesentery along with the pronounced median effective concentrations (EC₅₀) of 3.12 ± 0.26 and 2.40 ± 0.40 μM, respectively among the two hundred natural compounds [Luna-Vázquez et al. 2013].

Other than the ordinary NO synthase pathway present in the vascular endothelium, the attenuation of angiotensin converting enzyme found as the possible mechanism was demonstrated by **4** (page 6) in lowering the blood pressure [Riche et al. 2014]. Akinwumi [2017] reported that the *in vitro* and *in vivo* capabilities of **3**, **4** and **5** (page 6) in suppressing cardiomyocyte hypertrophy and enhancing diastolic function were more noticeable in spontaneously hypertensive rat (SHR) compared to spontaneously hypertensive heart failure (SHHF) rats. They suggested that the stilbene derivatives could be the suitable medications for human cardiovascular diseases. Clinical study demonstrated **3** that was utilized as the secondary prevention of myocardial infarction together with the routine medical therapy were able to improve the left ventricle diastolic and endothelial function of the patients with constant coronary artery disease in three months [Magyar et al.2012].

The complete vasorelaxation mechanism studies of **3** were done by Tan et al. in 2020. They concluded the vasorelaxation effects of **3** were attributed to the endothelium-derived relaxing factors (EDRFs) such as the PGI₂ and NO/sGC/cGMP pathways, followed by the G-protein-coupled β-adrenergic and muscarinic receptor pathways. The signalling pathways comprised both the potassium and calcium channels. Compound **3** could suppress not only the extracellular calcium influx, but

also the intracellular release of the calcium from the sarcoplasmic reticulum (SR) within the VSMCs.

Notably, there were only the *trans*- (E) isomers of stilbene derivatives had been studied their vasorelaxation activities and this could be due to most of the comparative studies revealed that *cis*- form was less reactive than the *trans*- form in various kind of biological activities [Szekeres et al. 2010; Cai et al. 2011; Nawaz et al. 2017; Savio et al. 2016].

1.7 Problem Statement

Although the *trans*-stilbene scaffold of stilbenoids and stilbenes derivatives had been proven for their potential in vasorelaxation activities of blood vessel, the complete structure-vasoactivity relationship of stilbene derivatives is still yet to be explored. The existing vasorelaxation studies focussed mainly on the derivatives of **3** with the 3-, 5- and 4'- positions of different substituents [Szekeres et al. 2010]. Various structural modifications of the *trans*- stilbene derivatives have been attempted but only with the other biological activities such as the *in vitro* studies focussed on the anti-cancer and anti-oxidant properties [Cai et al. 2011; Savio et al. 2016].

It was known that the methoxylated stilbene derivatives exhibited the higher bioavailability than that of the hydroxylated one although the latter exerted a more favourable vasorelaxant effect [Akinwumi at al. 2018]. Therefore, it is necessary to investigate the structural requirements of the *trans*- stilbene derivatives that are responsible in showing the *in vitro* vasorelaxation effect as the prerequisite for the subsequent studies of the vasorelaxation mechanism.

1.8 Objectives of the Research

The objectives of this research are:

- i. To synthesize and characterise *trans*- (*E*) stilbene derivatives with different numbers and types of substituents at different positions on the stilbene scaffold.
- ii. To investigate the vasorelaxation response of the synthesized *trans*- (*E*) stilbene derivatives.
- iii. To investigate the structure-vasoactivity relationships (SARs) of the synthesized *trans*- (*E*) stilbene derivatives.

1.9 Scope of Study

The *trans*- (*E*) stilbene derivatives were synthesised via the conventional Wittig reaction. The stilbene derivatives were devised wherein the substituents occupied 2,3-, 2,4-, 2,5-, 3,4-, 3,5-, 2-, 3-, and 4- positions of the aromatic rings. The substituents were adopted among ethoxy, methoxy and hydroxy groups. The hydroxylated stilbenes were only synthesized from the tri-ethoxy and tetra-methoxy stilbene derivatives via poly *O*-dealkylation. The chemical structures of the synthesized compounds was characterized by FT-IR (frequency of 4000 to 600 cm^{-1}), 1D- and 2D-NMR (500 MHz) spectroscopic techniques. The vascular response elicited by the synthesized compounds was conducted by using the *in vitro* method specifically on the endothelium-intact isolated aortic rings of the male SD rats. The vascular response data was obtained in quadruplicate (n=4) and expressed as the maximum relaxation value (R_{max}) that could be compared quantitatively with the lead compound, **RV**.

CHAPTER 2

METHODOLOGY

2.1 Materials

All the materials used were commercial sources retained without additional purification. Prior to the stilbene derivatives, the intermediates and Wittig reagents were synthesized according to methods published [Abell et al. 2004; Majeed et al. 2007; McNulty and McLeod 2013] with some minor modifications (Section 2.3). Table 2.1 and Table 2.2 list the types and sources of all the chemicals consumed in this study.

Table 2.1 List of chemicals used in the synthesis (Section 2.3).

Chemicals	Sources
2,3-Dihydroxybenzoic acid, 99%	ACRŌS ORGANICS, Belgium
2,3-Dimethoxybenzaldehyde, 98%	Sigma-Aldrich, UK
2,4-Dihydroxybenzoic acid, 97%	Sigma-Aldrich, UK
2,4-Dimethoxybenzaldehyde, 98%	ACRŌS ORGANICS, India
2,5-Dihydroxybenzoic acid, 98%	Sigma-Aldrich, UK
2,5-Dimethoxybenzaldehyde, 99%	Sigma-Aldrich, UK
3,4-Dihydroxybenzoic acid, 97%	ACRŌS ORGANICS, India
3,4-Dimethoxybenzaldehyde, 99%	Sigma-Aldrich, UK
3,5-Dihydroxybenzoic acid, 97%	ACRŌS ORGANICS, Belgium
3,5-Dimethoxybenzaldehyde, 98%	ACRŌS ORGANICS, Belgium
2-Ethoxybenzaldehyde, >97%	Sigma-Aldrich, China
2-Methoxybenzaldehyde, >98%	MERCK, China
3-Ethoxybenzaldehyde, 98%	Sigma-Aldrich, China
3-Methoxybenzaldehyde, 97%	Fluka Chemika, UK
4-Ethoxybenzaldehyde, >97%	Fluka Chemika, UK
4-Methoxybenzaldehyde, 99%	MERCK, China
Acetone, AR grade	Qręc, Malaysia
Aluminium chloride (anhydrous), >98%	MERCK, Germany

Table 2.1-2.1 Continued.

Chemicals	Sources
Bromoethane, 98%	Sigma-Aldrich, China
Dichloromethane, AR grade	Qręc, Malaysia
Diethyl ether, AR grade	Qręc, Malaysia
Ethanol 99.7%, AR grade	Qręc, Malaysia
Ethyl acetate, AR grade	Qręc, Malaysia
Methanol, AR grade	Qręc, Malaysia
<i>N,N</i> -Dimethylaniline, 99%	Sigma-Aldrich, China
Potassium carbonate (anhydrous), >99%	MERCK, China
Potassium iodide, >99 %	Sigma-Aldrich, China
Pyridine, 99.8%	Sigma-Aldrich, UK
Sodium borohydride, 99%	ACRÖS ORGANICS, Belgium
Sodium hydroxide, 99%	Qręc, Malaysia
Tetrahydrofuran, AR grade	Qręc, Malaysia
Thionyl chloride, >99 %	MERCK, Canada
Triphenylphosphine, >99 %	MERCK, China

Table 2.2 List of chemicals used in the bioassay (Section 2.4).

Chemicals	Sources
Acetylcholine chloride, >99%	Sigma-Aldrich, China
Calcium chloride dihydrate, >97%	MERCK, China
D(+)-Glucose (anhydrous), >99.5	HmbG Chemicals, Malaysia
L(-)-phenylephrine hydrochloride, >98%	Sigma-Aldrich, China
Magnesium sulphate heptahydrate, >99.5	MERCK, China
Potassium chloride, >99%	Sigma-Aldrich, China
Potassium dihydrogen phosphate, >99.5	MERCK, China
Sodium hydrogen carbonate, 99.5%	AnalaR, UK
Sodium chloride, >99.5%	R&M Chemicals, Malaysia
Tween 80	Sigma-Aldrich, China

2.2 Characterization of the Synthesized Compounds

All the qualitative characterizations of the synthesized compounds were performed using the scientific instruments at School of Chemical Sciences, USM.

2.2.1 *Melting points*

Melting points of the synthesized compounds were observed from the Gallenkamp MPA instrument without calibration. The closed end of the capillary tubes was filled with dry solid samples before the tubes were inserted into the oven block of the instrument and left to equilibrate. The range of reading was recorded once the samples started to melt and turned completely into the liquid form.

2.2.2 *Fourier Transform Infrared (FT-IR) Spectroscopy*

The infrared analyses of the samples were performed using the Attenuated Total Reflectance (ATR) technique by the Perkin Elmer 2000-FTIR spectrophotometer. The dry solid samples were placed on the ATR crystal plate before the gauge pressure of 97-99 units was applied. The FT-IR spectra were obtained in the range of 4000 to 600 cm^{-1} .

2.2.3 *Fourier Transform Nuclear Magnetic Resonance (FT-NMR) Spectroscopy*

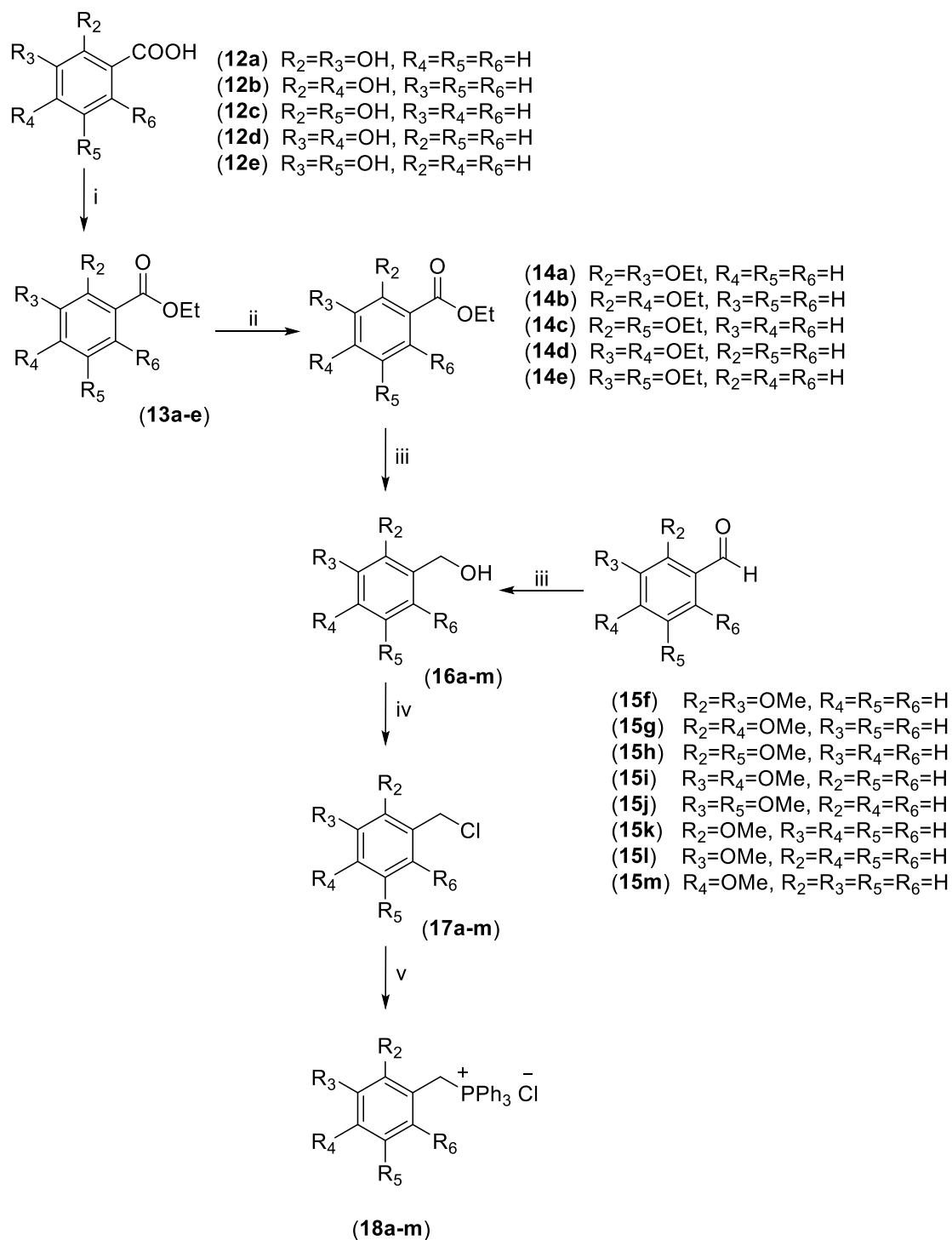
The NMR analyses of the samples were performed using a Bruker-Avance 500 MHz ultrashield spectrometer equipped with an autosampler. The samples were dissolved in 0.6 mL of deuterated solvent (CDCl_3 or DMSO-d_6) and transferred into the NMR tube. The NMR tube was inserted into the spinner with the adjusted depth gauge before placing into the autosampler. One dimensional (^1H NMR, ^{13}C NMR and ^{31}P NMR) and two dimensional (COSY, HMQC and HMBC) NMR spectra were obtained from the processing software. Chemical shifts (δ) for all NMR spectra were reported in parts per million (ppm) to remaining solvent protons. Coupling constants

(J) were calculated in hertz (Hz) and the peaks were observed as singlet (s), doublet (d), triplet (t), quartet (q), multiplet (m), doublets of doublet (dd), doublets of triplet (dt), triplets of doublet (td) and broad (br).

2.3 Synthesis of Stilbene Derivatives

The phosphonium salts, (**18a-m**) were synthesized according to the Scheme 2.1. The tri-substituted (**SB 1-7**), tetra-substituted (**SB 8-13**) and di-substituted (**SB 14-16**) stilbene derivatives were synthesized via the conventional Wittig reaction (Sections 2.3.2-2.3.4) from the phosphonium salts, (**18a-m**) and substituted benzaldehydes, which represented the A- and B-ring structures respectively, of the stilbene backbone (Table 2.3). **SB 1b-13b** were synthesized from **SB 1a-13a** via the poly *O*-dealkylation method [Majeed et al. 2007].

2.3.1 Synthesis of phosphonium salts (**18a-m**) from dihydroxybenzoic acids, (**12a-e**) and methoxybenzaldehydes, (**15f-m**)



Scheme 2.1 The synthesis of phosphonium salts, (**18a-m**). Reagents and conditions:

i) EtOH, H₂SO₄, reflux; ii) bromoethane, K₂CO₃, KI, acetone, reflux; iii) NaBH₄,

THF-MeOH, reflux; iv) SOCl₂, pyridine, r.t ; v) triphenylphosphine, THF, 120°C.